https://doi.org/10.5194/egusphere-2025-3173
Preprint. Discussion started: 4 August 2025

On the intensity and destructive potential of a past extreme, synoptic storm in a future warmer climate

Johanne Kristine Haandbæk Øelund[1, 2, 3, 4], Jens Hesselbjerg Christensen[1], Rune Magnus Koktvedgaard Zeitzen[2], Henrik Vedel[2], and Henrik Feddersen[2]

[1]University of Copenhagen, NBI, PICE, Copenhagen, Denmark
[2]DMI - Danish Meteorological Institute, Copenhagen, Denmark
[3]DTU Construct, Lyngby, Denmark
[4]DTU Management, Lyngby, Denmark

Correspondence: Johanne Kristine Haandbæk Øelund (johanne.oelund@nbi.ku.dk)

Abstract. The global climate is undergoing significant changes, with rising greenhouse gas concentrations driving increased temperatures, altered precipitation patterns, and sea level rise. Yet, the full implications for mid-latitude storm systems remain an area of active investigation. This study examines how such storms may intensify under future warming, focusing on Storm Anatol, which severely impacted Denmark on 3 December 1999. Using the high-resolution weather prediction model HARMONIE-AROME and a pseudo-global warming (PGW) framework, the storm is simulated under a range of thermodynamic conditions representative of a warmer climate.

Results show a clear warming signal, with increased near-surface temperatures and atmospheric moisture contributing to stronger storm dynamics. Wind and gust speeds rise systematically with temperature, while the spatial extent and duration of damaging wind conditions also expand. To quantify these changes, we introduce the Cumulative Wind Exposure Index (CWEI), which captures the integrated spatial and temporal severity of wind exposure.

Application of CWEI reveals a marked increase in cumulative wind exposure in warmer scenarios relative to the historical case. When linked to established wind-damage relationships, this translates to substantially higher potential for structural damage and disruption. These findings suggest that storms like Anatol, already destructive in the past, are likely to become even more damaging under future climate conditions. This underscores the need for climate-resilient building standards, improved early warning systems, and long-term adaptation strategies across northern Europe.

1 Introduction

High wind speeds related to the development of intensive extratropical low pressure systems, represent a significant socioeconomic and environmental hazard (IPCC, 2021). These intense weather events cause extensive damage to natural and managed systems, with the most immediate impact for humans being structural destruction due to high sustained wind speeds and, more critically, severe gusts (Gliksman et al., 2023). The forces resulting from the passage of such low-pressure systems can be very destructive (Little et al., 2023), e.g. tearing roofs from buildings, uproot trees, and bring down power lines, resulting in widespread infrastructure disruptions. Transportation networks are particularly vulnerable, with bridge closures, flight cancel-

https://doi.org/10.5194/egusphere-2025-3173
Preprint. Discussion started: 4 August 2025

lations, and railway disruptions leading to substantial economic consequences (Donat et al., 2011a). Additionally, storms are often accompanied by storm surges, which amplify the overall damage to the coastal regions (Souto-Ceccon et al., 2025; Woth et al., 2005).

According to EUROCODE (2005), the basic wind speed value, which should only be surpassed once in 50 years, in Denmark is set at 24 m/s across most regions, except within a marginal zone at the west coast of Jutland. In this zone, which includes areas within 25 km of the North Sea, the basic wind speed is 27 m/s at the coast, gradually decreasing to 24 m/s at the zone's inland boundary. Therefore, assessing whether current adopted wind speed design levels will be challenged in a warmer world is of considerable interest.

This study focuses on one of the most powerful storms recorded in Denmark: Storm Anatol, which struck on 3 December, 1999 (Nielsen and Sass, 2003). Anatol is classified as a storm based on widespread sustained wind speeds exceeding 24.5 m/s, a commonly used threshold for defining storm events. Anatol remains among the strongest storms measured by anemometers in Denmark [1], and its impact was profound. Although storms of this magnitude are relatively rare, their effects on society underscore the need for further investigation.

A key question arises: While no two storms events are identical, could a similar event become more intense in a warmer climate?

Future climate projections, such as those assessed by the Intergovernmental Panel on Climate Change (IPCC), indicate that with rising global temperatures, changes in precipitation, and the intensification of several types of extreme weather events are also to be expected. While the thermodynamic effects of warming (Lindsey and Dahlman, 2024; IPCC, 2021) and increased moisture (Christensen and Christensen, 2003) are well documented, significant uncertainty remains regarding the impact of climate change on extratropical storm intensity and frequency. Some studies, such as Bengtsson et al. (2009), suggest that while the intensity of individual storms may not increase significantly, there could be a rise in the number of storms exceeding 45 m/s in Northern Europe. Conversely, The WASA Group (1998) found no clear intensification of storms along the European coastline over the past century. There is currently no clear consensus regarding how wind patterns will evolve in a warmer climate. However, an increasing number of studies suggest a north–south contrast in future windstorm activity over Europe: northern regions, particularly around the North Sea and the British Isles, are projected to experience more frequent or intense wind events, while southern Europe may see either no significant change or a reduction in storm intensity (Ruosteenoja et al., 2019; Severino et al., 2024).

This study examines the potential intensification of extreme cyclones in a warming climate. Building on the work of Matte et al. (2022) and Zeitzen et al. (2025), the 1999 Storm Anatol, also known in Denmark as "December-orkanen" is analysed. No storm in Denmark exceeding its intensity has occurred since, although the storm Allan (2013) (von Storch et al., 2014) and the storm Erwin/Gudrun (2005) were close (Andrée et al., 2021).

[1]The storm Allan - October 28, 2013 - reached a mean wind speed of 39.5 m/s, but surpassed Anatol in Gust reaching 53.5 m/s (von Storch et al., 2014). This measurement was however made at a higher point at 17 m and therefore cannot be fully compared

https://doi.org/10.5194/egusphere-2025-3173
Preprint. Discussion started: 4 August 2025

The primary objective of this study is to assess whether a synoptic storm, like Anatol, could become more intense and disruptive in a warmer climate, while large-scale atmospheric conditions remain similar, by examining changes in mean wind speed and gust intensity and direction.

A storyline approach is employed (Shepherd et al., 2018), using a pseudo-global warming (PGW) method (Schär et al., 1996) to simulate Anatol under a future warming scenario. Event-based studies, such as this, are well suited for investigating how specific extreme events may respond to climate change (Trenberth et al., 2015). However, they pose certain challenges. Extreme storms are inherently unique, forming due to the precise alignment of multiple meteorological and climatological drivers (Ulbrich et al., 2009). When modifying atmospheric conditions to reflect a warmer climate, there is a risk of altering the storm's fundamental dynamics, potentially reducing its extremity rather than amplifying it (see e.g. Matte et al. (2022).

Importantly, this research does not assess whether the frequency of such events will increase in a future warmer climate, but rather investigates whether the intensity of an Anatol-like storms could be amplified under warmer conditions.

2 The storm Anatol, viewed from a Danish perspective

On 3 December, 1999, Storm Anatol impacted Denmark, southern Sweden and northern Germany, producing severe meteorological and hydrological consequences. Anatol developed rapidly over the eastern North Atlantic in early December 1999. Its formation was triggered by the interaction of two atmospheric disturbances, one at the surface moving northeast from Newfoundland and another in the upper atmosphere from Labrador. By the evening of 2 December, a closed surface low had formed west of Ireland, moving eastward along the southern edge of a cold upper-level trough centered over Iceland, see e.g., Ulbrich et al. (2001).

Anatol intensified quickly in a zone of strong temperature contrasts, with warm air to the south and exceptionally cold air to the north. By early 3 December, its central pressure had dropped to around 990 hPa near the British Isles and continued falling, reaching a minimum of 952 hPa over eastern Jutland at 1800 GMT. It then moved across Denmark into Sweden and began weakening after crossing the Baltic Sea (Voldborg, 2000; Ulbrich et al., 2001; Kettle, 2021; Nielsen and Sass, 2003). Figure 1 illustrates the modeled trajectory of the storm, based on the simulations from HARMONIE-AROME.

The storm's strongest winds occurred south of its center, affecting areas from the German and Danish North Sea coasts to Copenhagen and Poland. Denmark experienced widespread gale force winds and in the southern part of the country sustained winds reached storm force (>24.5 m/s), with peak gusts exceeded hurricane force (>40 m/s) in exposed coastal areas from 1400 to 2200 GMT, peaking between 1600 and 1800 GMT with the passage of the cold front (e.g., Zeitzen et al. (2025)).

Anatol produced record-breaking wind speeds. During the event, 10-minute mean wind speeds exceeded 41.4 m/s, before the anemometer at Rømø failed, with gusts reaching 51.4 m/s onshore (Cappelen et al., 2018), categorizing it as a 100 year event (Kettle, 2021). The offshore Mærsk Endeavour oil rig recorded a gust of 59.2 m/s at 40 m above mean sea level. Additional wind measurements included gusts of 41 m/s at Copenhagen Airport and 40 m/s on the island of Bornholm (Cappelen et al., 2018).

https://doi.org/10.5194/egusphere-2025-3173
Preprint. Discussion started: 4 August 2025

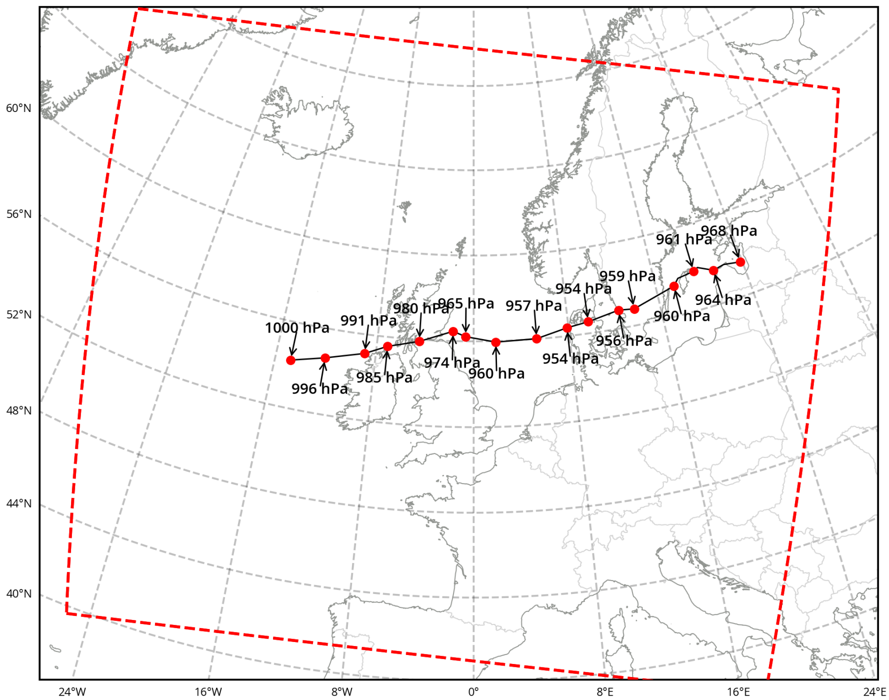

Figure 1. The track of the modeled Storm Anatol, indicating the minimum pressure and location of the storm at 2-hourly intervals from 2 December 2200 UTC ending at 4 December 0600 UTC. Red dashed lines delineates the HARMONIE model domain.

The storm caused 800 injuries and 7 fatalities in Denmark, airports were closed, and transport greatly interrupted (Kettle, 2021). Approximately 4 million m^3 of forest was damaged. Storm Anatol caused extensive damage to buildings, including the collapse of a large crane at the Odense shipyard. Widespread power outages occurred across Denmark, and the total economic loss was estimated at 1.7 billion EUR, which, adjusted for inflation, corresponds to approximately 2.8 billion EUR in 2024 (Cappelen et al., 2018; Kettle, 2021). In Germany the storm losses reached 100 million EUR (Klawa and Ulbrich, 2003) and in Sweden 5 million m^3 of forest were damaged (Nilsson et al., 2007).

Given its intensity and extensive societal impact, Storm Anatol serves as a compelling case study for assessing the potential effects of a warmer climate on storm intensity.

Denmark was selected as the focus of this study because the storm had a particularly severe impact on the country, and detailed documentation of the storm severeness and resulting damages is readily available.

3 Theory

Extratropical cyclones develop and intensify primarily due to baroclinic instability, a process driven by the conversion of available potential energy (APE) into kinetic energy (Federer et al., 2025). This mechanism is fundamental to the growth of

https://doi.org/10.5194/egusphere-2025-3173
Preprint. Discussion started: 4 August 2025

midlatitude weather systems and is well-documented in meteorological literature (e.g., Catto, 2016). APE is generated from the temperature gradients in the troposphere, with stronger gradients providing more energy for cyclone growth. Baroclinic instability is a key mechanism for the development of such cyclones (Eady, 1949).

Additionally, latent heat release from phase changes in atmospheric moisture can contribute to cyclone intensification. The release of latent heat during condensation warms the atmosphere, reducing static stability and enhancing upward motion, which can further intensify cyclonic systems (Li et al., 2014). Furthermore, studies have shown that the rapid intensification of Anatol was strongly influenced by latent heat release (Kettle, 2021; Zeitzen et al., 2025). This process has been identified as a significant factor in the explosive deepening of extratropical cyclones (Fink et al., 2012).

The availability of APE is proportional to temperature variations within the troposphere, which explains the increased frequency and intensity of extratropical cyclones during the winter months, when temperature gradients are typically more pronounced. Stronger temperature gradients enhance baroclinic instability, providing more energy for cyclone development and intensification (Laurila et al., 2021; Ulbrich et al., 2009).

Since the early 1980s, reports have suggested an increasing trend in storm events over the North Atlantic region, although the available data covered only a short time frame (Neu, 1984). This trend raised concerns about a possible link to climate change (The WASA Group, 1998). Feser et al. (2015) identified an increasing trend in storm activity over northern Europe and the North Atlantic, while noting a negative trend over southern Europe. Future climate projections indicate a rise in storm frequency during the winter months over the North Atlantic and Western Europe (Della-Marta and Pinto, 2009). However, these projections are highly dependent on the climate models used, with variations in the predicted magnitude and spatial distribution of storm activity (Chang et al., 2022). Some models project an increase in cyclonic activity over regions like the British Isles and Denmark, while others suggest decreases in different areas, highlighting the uncertainties inherent in such projections (Little et al., 2023). Similarly, Gastineau and Soden (2009) found that global warming is expected to reduce the frequency of extreme winds in the tropics while increasing their occurrence in the extratropics. This pattern appears to be strongly linked to the intensification and poleward shift of midlatitude storm tracks.

4 Methodology, model and Data

Storm Anatol has been the subject of extensive analysis in both meteorological literature and media reporting due to its severe impact across Northern Europe (Kettle, 2021; Ulbrich et al., 2001). In the present study, the storm is re-evaluated using the HARMONIE-AROME limited-area numerical weather prediction (NWP) model to explore its sensitivity to varying temperature conditions. A historical 1999 reference simulation (control run) is conducted, using conditions taken from ERA5 alongside four additional experiments in which the atmospheric temperature is systematically perturbed by $+1°$ C, $2°$ C, $+3°$ C, and $-1°$ C. These perturbations are applied throughout the entire atmosphere in the initial and boundary conditions. These modifications aim to emulate plausible future warming scenarios as well as approximate preindustrial (PI) climatic conditions (IPCC, 2021b). The validation of the model data is described in Zeitzen et al. (2025).

https://doi.org/10.5194/egusphere-2025-3173
Preprint. Discussion started: 4 August 2025

4.1 Harmonie Model and data

The simulations are carried out using the HARMONIE-AROME weather model (Bengtsson et al., 2017) based on cycle 43h2.2. The utilised model setup has a horizontal resolution of 2 km with 90 vertical levels between the surface and 10 hPa (approximately 25 km above sea level), capturing mesoscale atmospheric processes with high fidelity.

A model setup similar to that used operationally by the United Weather Centres West (comprising Denmark, Iceland, the Netherlands, and Ireland) is adopted, featuring a broad domain extending into the North Atlantic, see Figure 1. This wide coverage enables extended simulation of the cyclone under PGW-modified conditions. The model is run without data assimilation, as the event is primarily driven by large-scale upper-level atmospheric dynamics.

Initial conditions and lateral boundary data are derived from the ERA5 reanalysis (Hersbach et al., 2020), with boundary updates every 3 hours. The initial forecast is started from an interpolated ERA5 analysis, while each subsequent run is started using the +6-hour forecast from the prior cycle to mitigate spin-up issues.

As detailed in Zeitzen et al. (2025), each simulation consists of 11 forecast cycles, initiated every 6 hours over the period 01–03 December 1999, each providing a 24-hour forecast. Model output is saved at hourly intervals, except for wind speed, which is stored every 15 minutes to capture short-term variability and peak intensities.

The control simulation uses unmodified ERA5 temperatures, while the anomaly runs incorporate uniform perturbations throughout the model domain. To produce a temporally consistent time series of the storm's life-cycle, a mosaic is compiled using the model output from forecast hours +09 to +14 from each run. This method ensures continuous hourly coverage during the most dynamically active phase of the cyclone. Further details on the HARMONIE-AROME model setup and physics can be found in Bengtsson et al. (2017) and Zeitzen et al. (2025).

4.2 Pseudo-global warming and story-line approach

The Pseudo-global warming approach is a widely used method for assessing the potential impact of climate change on extreme meteorological events. The technique involves modifying the thermodynamic state of the atmosphere while preserving the original dynamical weather setup. Specifically, this is done by uniformly adjusting air temperature at all levels and then recalculating specific humidity to maintain the original relative humidity, thus emulating a warmer and moister climate (Brogli et al., 2023).

This approach allows retaining the essential structure of the meteorological phenomenon while examining how it responds to systematic climate shifts. Here, temperature modifications of $-1°$ C, $+1°$, $+2°$ C and $+3°$ are applied to the Initial Conditions and Lateral Boundary Conditions, as well as to skin temperature and sea surface temperature that are used by the weather model. The procedure for adjusting specific humidity is detailed in Zeitzen et al. (2025). These modified simulations are directly compared with an unmodified reference run, providing a controlled basis for analysing changes.

The $-1°$ C simulation approximates a pre-industrial climate state (IPCC, 2021a), while the $+1°$ C to $+3°$ C runs represent plausible future warming scenarios. These enable us to evaluate how Anatol's wind intensity and related impacts might change under increasing global temperatures, within a storyline framework (Shepherd et al., 2018).

https://doi.org/10.5194/egusphere-2025-3173
Preprint. Discussion started: 4 August 2025

The use of spatially and vertically uniform perturbations is informed by prior studies (Hibino et al., 2018; Matte et al., 2022), which showed that PGW scenarios derived from general circulation model (GCM) outputs can unintentionally alter the dynamics that originally produced the extreme event. Such alterations can dampen the intensity of the simulated extremes, thereby reducing the realism of the modified future scenarios (Matte et al., 2022).In addition sensitivity tests (not shown here) were conducted on vertical temperature lapse rates and the overall large-scale north-south temperature gradient. These experiments further confirmed that overly smoothed thermodynamic changes may reduce the storm system's dynamic response, again consistent with findings by Hibino et al. (2018) and Matte et al. (2022).

The storyline approach is particularly valuable for this type of analysis. Rather than focusing on probabilistic outcomes, it provides a set of physically self-consistent "what-if" scenarios for a known extreme event. By comparing modified simulations with the reference run, addressing whether increased or decreased wind intensity is plausible and identify the mechanisms responsible can be explored. This method helps isolate primary and secondary processes driving the storm's behavior—processes that might otherwise be overlooked due to the complex, multiscale nature of mid-latitude cyclones (Zeitzen et al., 2025).

Importantly, the scientific validity of this method depends on the quality of the reference run. If the reference accurately replicates the observed event, the sensitivity simulations remain physically coherent and offer insights into how the same system might evolve under different climate conditions (Ciullo et al., 2021). As demonstrated in Zeitzen et al. (2025), in part due to the high resolution of the simulations. The reference run conducted with HARMONIE-AROME compares very well with observation, in particular sustained wind speeds and gusts are depicted realistically.

An added strength of the storyline framework is its relevance for science communication. By anchoring abstract climate scenarios in a real and impactful historical event, it helps translate scientific insights into terms that are tangible and relatable—highlighting the potential effects of climate change in ways that inform both public awareness and policy-making (Sillmann et al., 2021; Shepherd, 2019).

4.3 Cumulative wind exposure index (CWEI)

To assess the severity of a storm, it is essential to consider not only the peak wind speed but also the duration of high wind conditions, as prolonged exposure can significantly affect the structural integrity of materials (Lynn and Stathopoulos, 1985; Wang et al., 2024). In addition, the total economic loss associated with a storm is closely linked to the spatial extent of the impacted area (Grinsted et al., 2019). To capture these combined effects, a simple index is introduced that integrates wind intensity, duration, and spatial coverage.

In this study, storm severity is quantified using a Cumulative wind exposure index (CWEI), which accounts for both the spatial extent and the duration of wind speeds exceeding a chosen damage threshold. The CWEI is defined as the cumulative sum of grid points and the time steps where wind speeds exceed a predefined limit, normalized by that threshold:

$$CWEI = \sum_{t=1}^{T} \sum_{(x,y)} 1(W_{t,x,y} > W_{thresh}) \tag{1}$$

https://doi.org/10.5194/egusphere-2025-3173
Preprint. Discussion started: 4 August 2025

$W_{(t,x,y)}$ denotes the mean wind speed at time t at the location (x,y), W_{thresh} is a predefined threshold, $1(\cdot)$ is the indicator function, equal to 1 if condition is true otherwise 0.

While a number of storm severity indices have been developed (e.g., Leckebusch et al. (2008), Gliksman et al. (2023)), many are designed for climatological analysis and rely on percentile-based thresholds, such as the 98th percentile of wind speeds. These are useful for statistical consistency across time and space, especially when comparing model output or reanalysis across long periods.

However, percentile-based thresholds may be less intuitive from an economic or engineering perspective, where losses and structural damage are tied to fixed, absolute wind speeds. Insurance claims, for instance, are typically triggered when gusts exceed regionally defined thresholds—not percentiles. In much of Europe, 24.5 m/s is used as a benchmark for storm events relevant to loss modeling and payout eligibility.

Additionally, from a constructional perspective, structural standards such as the EUROCODE (2005) specify characteristic wind actions based on expected maximum gusts, not relative thresholds. By aligning the CWEI formulation with such fixed values, the metric offers a more practically grounded assessment of storm severity—especially for applications related to infrastructure risk, adaptation planning, and insurance exposure.

The CWEI should therefore not be seen as a replacement for existing indices but rather as a complementary tool that integrates wind magnitude, spatial impact, and duration into a single, transparent metric tied to real-world damage criteria. Its simplicity and adaptability make it especially suited for single-event sensitivity studies such as this one.

4.4 Storm damages

Extreme wind events are inherently destructive due to the physical relationship between wind speed and the force exerted on structures. The kinetic energy of the wind, which scales with the square of the velocity (v^2) , provides a basic physical foundation for understanding storm impacts (Lorenz et al., 2024). However, when assessing actual damage and economic losses, especially those reflected in insurance data, the relationship between wind speed and financial loss is often found to be steeper than v^2.

Empirical studies have shown that insured losses frequently scale with higher powers of wind speed. For example, a cubic relationship (v^3) has been used in several risk assessment models (Donat et al., 2011b), while others support a quartic or quintic dependency (v^4–v^5), especially for modelling storm losses over Europe and North America where building exposure is high (Klawa and Ulbrich, 2003). These mid-range exponents are commonly applied in insurance and reinsurance models aiming to estimate aggregate losses over large regions with varying building codes and vulnerability profiles.

In contrast, higher-order exponents such as v^8 to v^{12} have been used in contexts where the focus is on local or asset-specific damage, particularly in engineering-focused studies that simulate wind loading on structures or consider total failure scenarios (Prahl et al., 2012). These exponents reflect the compounding effects of high winds on exposed infrastructure, where small increases in wind speed can disproportionately escalate the damage.

https://doi.org/10.5194/egusphere-2025-3173
Preprint. Discussion started: 4 August 2025

The choice of exponent is therefore context-dependent: lower exponents (v^2–v^3) capture general physical forces, moderate exponents (v^4–v^5) are often applied in large-scale insurance risk models, and higher exponents (v^8–v^{12}) are reserved for detailed local assessments or engineering design considerations.

5 Results

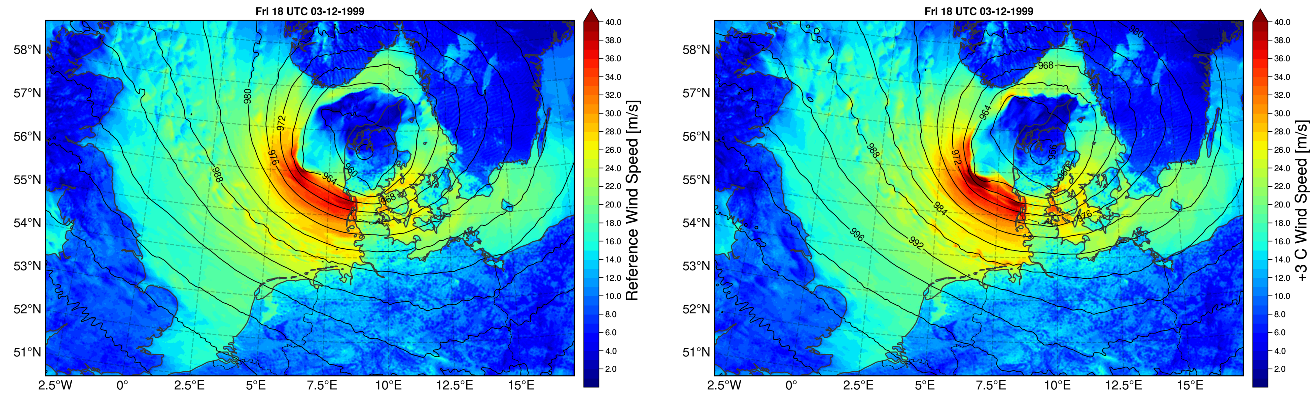

(a) Storm at UTC 18, control run

(b) Storm at UTC 18, $+3^\circ$ C Run

Figure 2. The storm intensity and low pressure system at 3 December, 1800 UTC, when the storm made landfall for each of the different model runs of the Control run and $+3^\circ$ C. The plots for the other runs of -1° C, $+1^\circ$ C and $+2^\circ$ C are shown in appendix A.

To assess the potential impact of a warmer counter-factual climate on extratropical cyclones, the storm Anatol was simulated under different temperature scenarios using the HARMONIE-AROME limited-area NWP model. This study primarily focuses on the difference observed between the control run and the $+3^\circ$ C warming scenario.

In terms of intensity and structure, the storm event is well reproduced by the HARMONIE model, Figure 2. This figure shows the modeled 10 m mean wind speed and msl at 1800 UTC, just before the storm makes landfall. The spatial structure of the control run, Figure 2a and the $+3^\circ$ C model run, Figure 2b are broadly similar. However, the $+3^\circ$ C run displays visibly stronger wind speeds, indicated by the darker red shading. Notably, the center of the low-pressure system shifts eastward with each degree of warming, but there is only an modest deepening of the central pressure from 954 hPa to 952 hPa. The modeled winds from the control run are generally similar to, though slightly higher, than the in-situ measurements from the actual event, providing validation for the models output (see Zeitzen et al. (2025)).

Table 1 presents the maximum wind speeds from within the entire model domain, for both mean and gust wind components. The overall intensity of the storm increases by roughly 0.6 m/s per degree of warming for mean wind speed, with a moderately strong linear relationship (R^2=0.78). For gust, the increase is about 0.7 m/s per 1°C of warming, though the fit is weaker (R^2=0.58). These trends, illustrated in Figure 3, highlighting a potential amplifying effect of a warmer climate on storm events.

https://doi.org/10.5194/egusphere-2025-3173
Preprint. Discussion started: 4 August 2025

Table 1. Overview of the maximum mean wind velocity and wind gust over land reached by each scenario.

	-1° C	Ref	$+1^{\circ}$ C	$+2^{\circ}$ C	$+3^{\circ}$ C
Max mean velocity	44.5 m/s	44.2 m/s	45.9 m/s	45.6 m/s	46.7 m/s
Max gust velocity	58.9 m/s	60.1 m/s	62.2 m/s	60.2 m/s	62.5 m/s

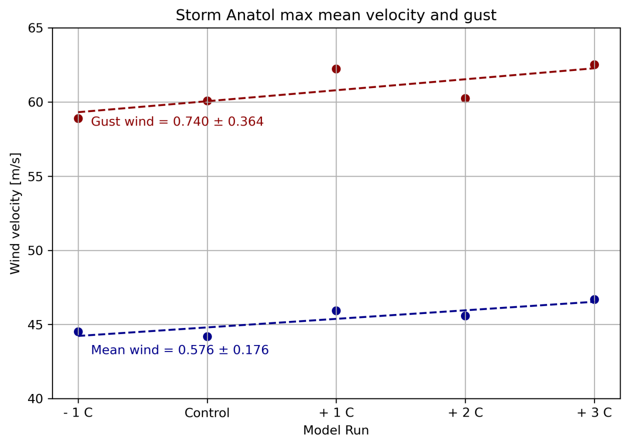

Figure 3. Increase of absolute maximum wind speed pr degree of warming.

This increase in maximum wind speed results in an increase in wind pressure on constructions in terms of kinetic energy with $11.7\ \%$ and a power increase of $18\ \%$. The empirical large scale insurance risk model increases in the range of $24.7\ \% - 31.8\ \%$ and the higher detailed assessment increases by $55.6\ \% - 94.1\ \%$. These values are calculated based on the various methods described above.

Figure 4 illustrates the duration of land area affected by wind speeds equal to or exceeding storm-force (e.g. 24.5 m/s), emphasizing the substantial impact of Anatol on southern Denmark. In the control run (Figure 4a) storm-force winds persisted in the western part of the country for up to eight hours. In contrast, the $+3^{\circ}$ C scenario (Figure 4b), the storm remained active for nine hours in some areas.

In figure 5 the time lapse for land areas experiencing either an increase or decrease in the period exceeding storm force over the area is presented. The northern part of the storm-area seems to experience a decrease in the storm-period from the control run to the $+3^{\circ}$C run, whereas the middle and southern part of the area affected experiences an increase in the storm period of up to 3 hours. $10\ \%$ of the affected area experiences an increase compared to $4.2\ \%$ that will experience a decrease. This is likely attributable to a slight change in the storm track, with the core wind field shifted slightly southward, suggesting that the reduction in duration may be an artifact of individual model realizations.

Furthermore, the percentage of land affected by wind speeds exceeding 24.5 m/s increases from $18.4\ \%$ in the control run to $21.5\ \%$ in the $+3^{\circ}$ C scenario, a difference of approximately 1500 km^2, as described in Table 2. Also shown in the table are

https://doi.org/10.5194/egusphere-2025-3173
Preprint. Discussion started: 4 August 2025

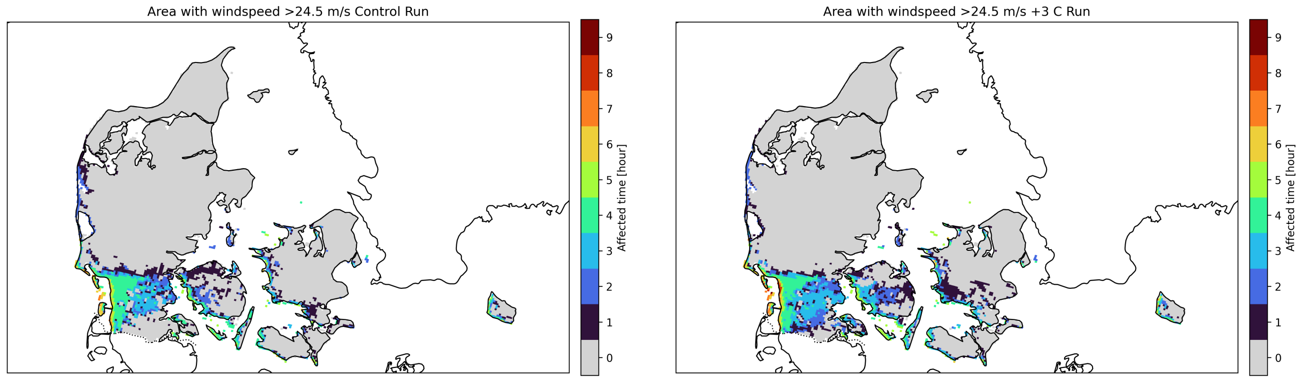

(a) Storm affected land for the control run

(b) Storm affected land for the $+3^{\circ}$ C model run

Figure 4. Time of which Danish land affected by wind above 24.5 m/s for the control run and the $+3^{\circ}$ C. The colourbar indicates the time each grid point experiences storm.

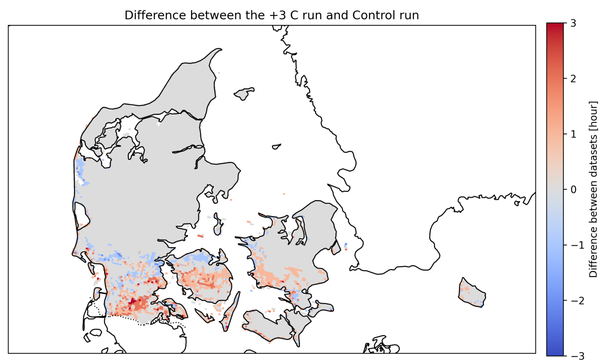

Figure 5. Areas that experience variations in the duration of storm.

the CWEI values for each scenario at particular wind speed thresholds. Similarly, for gusts exceeding 40 m/s[2], the impacted area rises from 29.5 % in the control run to 32.5 % in the $+3^{\circ}$ C scenario, shown in appendix B1. The full range of coverage percentages for different thresholds (from 15 m/s to 24.5 m/s) is provided in the appendix, Table C1.

Consequently, Anatol's CWEI increases by approximately 800 km^2h, per degree of warming for strong mean wind speeds (24.5 m/s), with a strong linear fit (R^2=0.81) as shown in Figure 6.

Figure 7 illustrates the temporal development of the maximum wind speed across all five scenarios. Figure 7a shows that the realised maximum wind speed is generally higher in the warmer scenarios, all exceeding 45 m/s. The control run and the simulation mimicing preindustrial (PI) conditions exhibit similar behaviour. However, the PI run reaches a slightly higher peak wind speed. This may be due to the -1° C perturbation modifying pressure gradients, static stability, or baroclinicity in a

[2] 40 m/s is often treated as a significant threshold for very dangerous situations

https://doi.org/10.5194/egusphere-2025-3173
Preprint. Discussion started: 4 August 2025

Table 2. Overview of the percentage of land affected by wind speed above 24.5 m/s at different durations, the total percentage of land that experienced storm and CWEI. An extended version is presented in appendix table C1, displaying the results for various thresholds.

	$-1°$ C	Ref	$+1°$ C	$+2°$ C	$+3°$ C
1 Hour	5.84 %	5.69 %	6.75 %	6.66 %	6.38 %
2 Hours	3.52 %	3.58 %	4.47 %	5.01 %	4.26 %
3 Hours	3.34 %	3.40 %	5.75 %	4.74 %	5.39 %
4 Hours	4.32 %	3.94 %	3.05 %	3.34 %	3.34 %
5 Hours	1.03 %	0.98 %	1.04 %	1.12 %	1.26 %
6 Hours	0.51 %	0.67 %	0.51 %	0.63 %	0.61 %
7 Hours	0.08 %	0.10 %	0.18 %	0.29 %	0.24 %
8 Hours	0.02 %	0.01 %	0.06 %	-	0.03 %
Total cover	18.65 %	18.37 %	21.81 %	21.78 %	21.51 %
CWEI [grid point]	5256	5191	5895	5954	6035

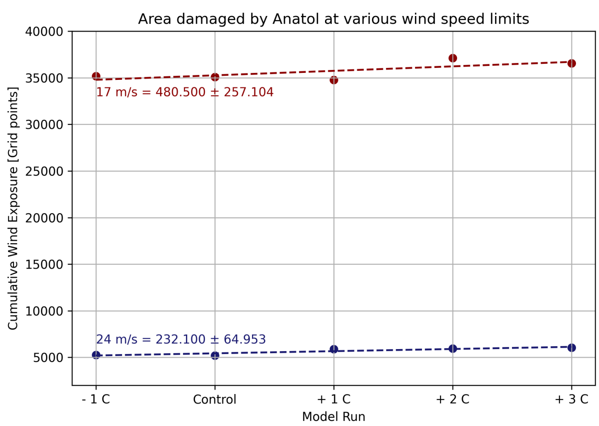

Figure 6. Development of the CWEI for the 5 modelled scenarios

https://doi.org/10.5194/egusphere-2025-3173
Preprint. Discussion started: 4 August 2025

way that locally enhances wind speeds, despite the overall reduction in thermal energy. The cooler perturbation may also have altered the storm's trajectory or internal structure, resulting in locally stronger winds than in the control run.

The timing of peak wind speeds varies among the scenarios. The $+2°$ C and $+3°$ C runs peak later, around 18–19 UTC, while the $+1°$ C, control, and $-1°$ C runs peak slightly earlier, at 17–18 UTC. Such variations might be expected, as even minor perturbations, including cooling, can influence storm intensity, position, and timing, particularly in mesoscale models where feedback processes are highly sensitive.

Figure 7b presents the proportion of land area affected by wind speeds exceeding 24.5 m/s. A clear trend emerges in which the affected area increases with warming. The control and PI runs show nearly identical behaviours, whereas all three warming scenarios exhibit a consistent increase in the affected land area throughout the storm's evolution. Notably, the maximum land area experiencing storm force winds occurs simultaneously for all three warming runs.

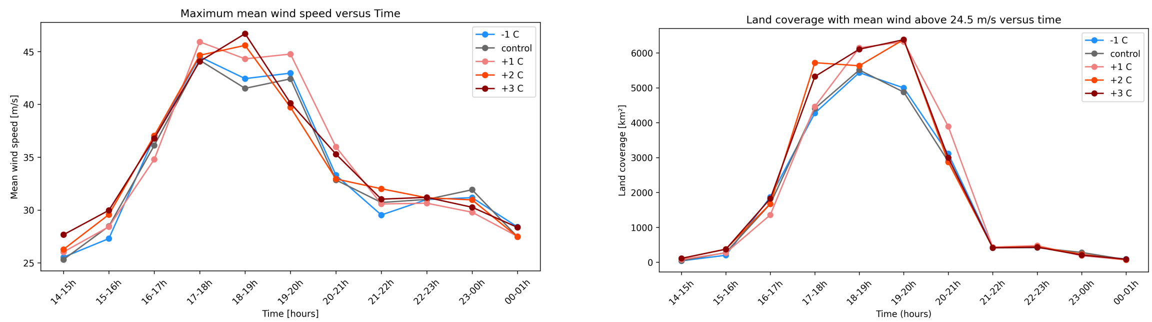

(a) Temporal variation of maximum mean wind velocity across the five scenarios.

(b) Distribution of land cover in percent across time slots for the five scenario simulations.

Figure 7. The time evolution of the maximum wind speed over land and the land affected by mean wind speed above 24.5 m/s.

In all scenarios, the wind directions consistently exhibits a westerly to south-westerly direction. The highest wind velocities tend to be more south-westerly (Figure 8c and 8d) compared to the overall wind field (Figure 8a and 8b). Notably, wind direction—when combined with coastal orientation and the layout of infrastructure—can influence vulnerability.

6 Discussion

The simulation of Storm Anatol under varying temperature scenarios reveals a clear intensification of the event with warming. Across all scenarios, increases in both mean wind speeds and gusts were identified, alongside an expansion in the spatial footprint of storm-force winds and a lengthening of the storm's duration. These changes are all associated with enhanced potential for infrastructural damage and societal disruption, emphasizing the importance of understanding how extratropical cyclones may evolve in a warming climate.

The trend of approximately 0.6 m/s per $1°C$ warming identified in this study is consistent with the findings of Hawkins et al. (2023) of 1 m/s pr 2 K in their simulation of the historical storm Ulysses.

https://doi.org/10.5194/egusphere-2025-3173
Preprint. Discussion started: 4 August 2025

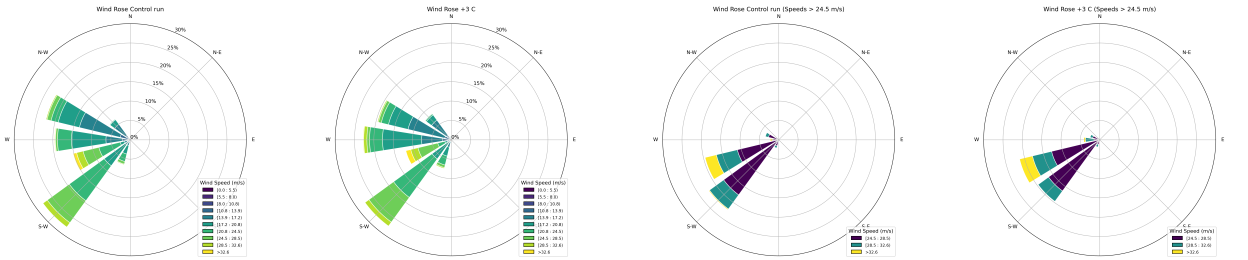

(a) Control run. (b) The +3° C run. (c) Control run > 24.5 m/s. (d) The +3° C run > 24.5 m/s.

Figure 8. Windrose displaying the wind direction for the two scenarios for all mean wind velocity and mean wind velocity above 24.5 m/s respectively. The data used is for the maximum values over land.

The observed increase in the land area affected by storm-force winds is consistent with previous findings. Priestley and Catto (2022) found that under high-emission scenarios such as SSP5-8.5, the area exposed to extreme storms could increase by as much as 40 % by the end of the century. While the present study does not reach that magnitude, it confirms the general trend toward spatial expansion of storm impacts under warming conditions, even in a single-event simulation. It is important to note, however, that the studies are not directly comparable on a one-to-one basis. Priestley and Catto (2022) assessed long-term climate model means, whereas this study examines a high-resolution simulation of a single storm event. Nevertheless, the alignment in trends strengthens confidence in the broader signal of increasing storm exposure with warming.

While the results are internally consistent and robust for Anatol, generalizations should be made cautiously. To confirm whether the trends identified here hold across a range of storm types and trajectories, future research should include simulations for multiple extreme wind events. This would enable a more systematic evaluation of the temperature sensitivity of extratropical cyclones.

It is important to acknowledge the limitations of regional NWP modeling, including uncertainties related to initial conditions, boundary forcing, and physical parameterizations. These factors may influence the simulated storm structure and intensity. Thus, proper model validation is key to be able to interpret sensitivities, such as in this study.

The societal implications of intensifying windstorms are substantial. Storms like Anatol disrupt energy and transportation infrastructure, endanger lives, and strain emergency response systems. The findings suggest that even moderate warming can amplify these hazards by increasing wind intensities, enlarging the affected area, and prolonging exposure to damaging conditions. Given that wind-related damages scale nonlinearly with wind speed—often approximated as proportional to v^{α}, where α can reach up to 12 for structural impacts, even modest increases in wind speed may translate into disproportionately large increases in damage potential. These risks call for integration of climate projections into national preparedness strategies, coastal infrastructure planning, and building codes.

Additional research is essential to build upon these findings. Simulations of other notable storms affecting Denmark and Northern Europe could assess the consistency of warming-induced intensification across different cases. Furthermore, integrating hydrodynamic models would provide valuable insights into how altered wind patterns may affect storm events, storm surges

https://doi.org/10.5194/egusphere-2025-3173
Preprint. Discussion started: 4 August 2025

and coastal flooding risk—an especially important consideration for low-lying and exposed regions. This study also does not address potential changes in storm frequency, which remain important but uncertain aspects of climate change impacts. These areas represent key directions for future investigation.

Finally, while much climate research has concentrated on changes in precipitation and flooding, less attention has been devoted to how climate change may affect the severity of windstorms in mid-latitude regions. Some global climate models suggest shifts in storm intensity, frequency, and storm track location under warming, though uncertainties persist—particularly regarding cyclone genesis and path variability. It is also worth noting that had Anatol occurred in the fall instead of winter, when sea surface and atmospheric temperatures are typically higher, the impacts may have been even more severe. Such seasonal considerations merit further exploration in future modeling efforts. Exploring the role of seasonal timing may offer additional insights, as higher autumn sea surface temperatures and increased atmospheric moisture could further amplify storm intensity and related impacts.

7 Conclusions

While it is not possible to attribute individual weather events to anthropogenic climate change in a strictly deterministic sense, advances in event attribution science, notably through efforts such as the World Weather Attribution (WWA) initiative (e.g., Philip et al. (2020)), have demonstrated that the likelihood and severity of many extreme events, such as heatwaves, droughts, and intense rainfall, have been significantly influenced by human-induced global warming.. Extratropical cyclones such as Storm Anatol result from complex interactions involving atmospheric circulation patterns, boundary layer dynamics, and surface conditions. A warmer climate influences many of these background factors, thereby increasing the potential intensity and spatial footprint of such events (Fischer and Knutti, 2015). This study used the HARMONIE-AROME limited-area model to examine how Storm Anatol might respond to warmer temperature scenarios. The simulations consistently show that increased temperatures lead to stronger winds, both in terms of mean wind and gust, longer storm durations, and larger areas affected by storm-force winds. Although the magnitudes of change are moderate, the signal is robust across all wind thresholds examined, suggesting a strong link between temperature and key storm severity metrics. Importantly, capturing these changes in storm structure and intensity requires the high spatial and temporal resolution provided by the NWP model, which exceeds that of typical climate model simulations and allows for more detailed representation of mesoscale dynamics and extreme wind events.

These findings are consistent with broader modeling literature indicating that intense extratropical storms are likely to become more intense and expansive under climate change. While the analysis is limited to a single storm, the results underscore the growing risks to public safety and critical infrastructure, even in regions where windstorms are already a familiar hazard.

This study contributes to the growing body of evidence that climate change is likely to exacerbate the impacts of extreme wind events. A more comprehensive understanding of these changes, both in terms of intensity and potential shifts in frequency or seasonal timing, is essential for informing adaptive strategies, improving early warning systems, and enhancing societal resilience to future storm extremes.

https://doi.org/10.5194/egusphere-2025-3173
Preprint. Discussion started: 4 August 2025

Ultimately, while this study cannot make probabilistic claims about future storm occurrences, it does contribute to the growing body of evidence that a warmer climate is likely to produce more impactful windstorms. Recognizing these patterns is crucial for informing adaptive planning and enhancing societal resilience to future extremes.

Appendix A: Wind

Figure A1 shows the five scenarios of Storm Anatol at 18:00 ETC, corresponding to its landfall. While the overall structure of the storm remains similar across the scenarios, an intensification of wind speed is evident, as indicated by the increasingly darker shades of red.

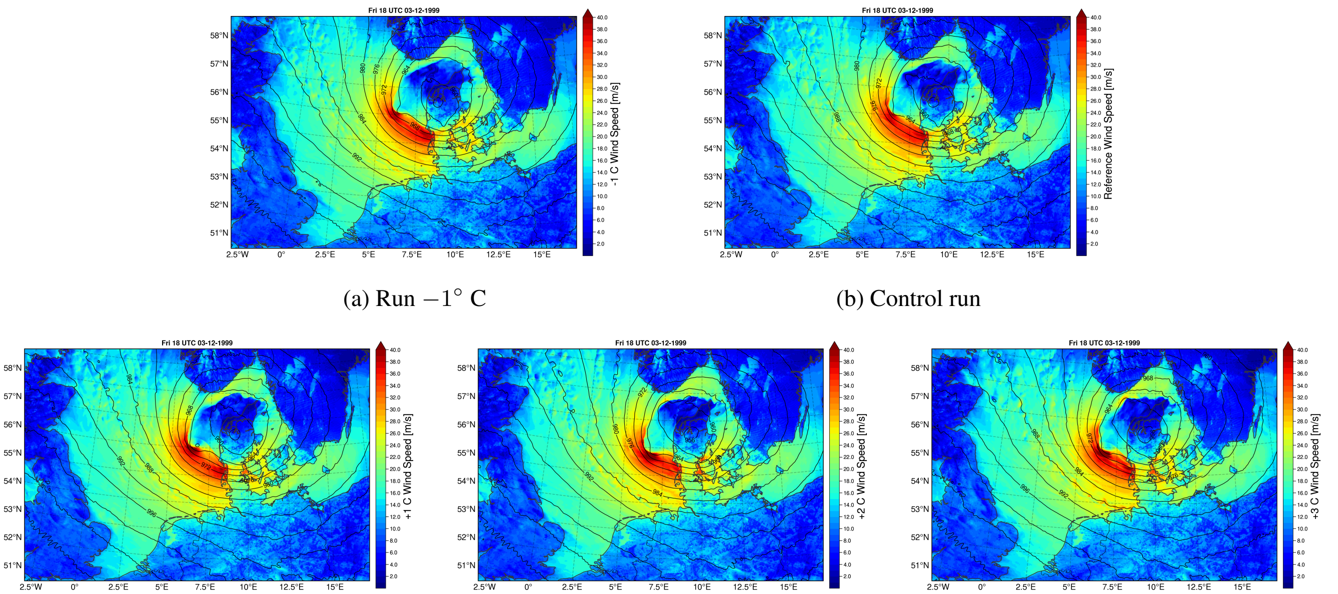

(a) Run -1° C

(b) Control run

(c) Run $+1^\circ$ C

(d) Run $+2^\circ$ C

(e) Run $+3^\circ$ C

Figure A1. The storm intensity and low pressure system at 3 December 1800 UTC, when the storm made landfall for each of the different model runs of -1° C, Control run, $+1^\circ$ C, $+2^\circ$ C and $+3^\circ$ C.

Appendix B: Gust

The land area affected by gust exceeding 40 m/s is shown in Figure B1. Although the variations are less pronounced than those observed for the wind-affected area, there is still a general increase in gust exposure, as illustrated in Figure B2. Severe gusts are especially pronounced in the southernmost part of Denmark in the warmer climate run.

https://doi.org/10.5194/egusphere-2025-3173
Preprint. Discussion started: 4 August 2025

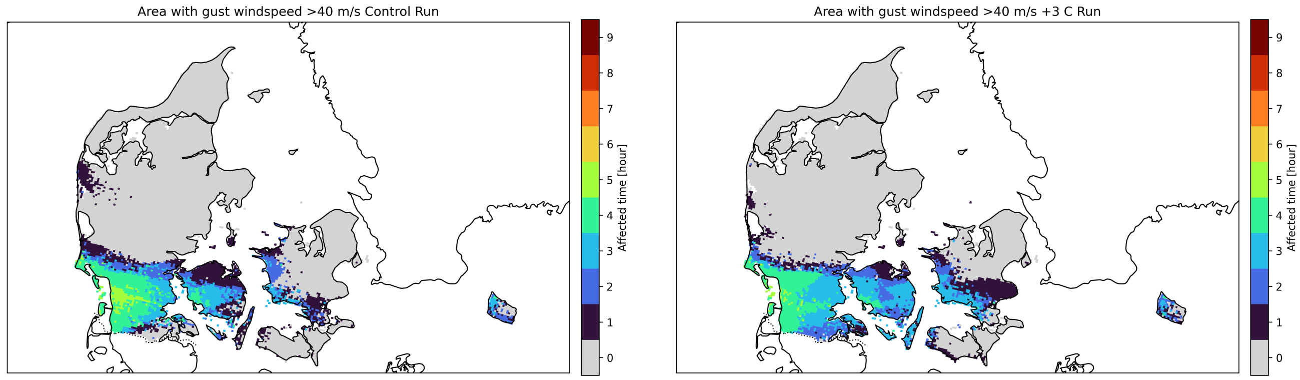

(a) Land cover for the control run

(b) Land cover for the $+3^{\circ}$ C

Figure B1. Time of which land is affected by gust above 40 m/s for the control run and the $+3^{\circ}$ C. The colourbar indicates the time each grid point experiences gust above 40 m/s.

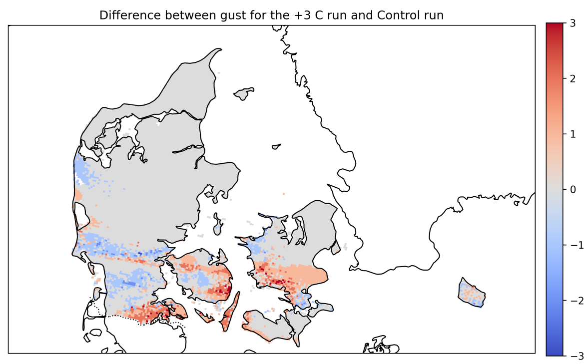

Figure B2. Area experiencing a variation in the duration of gust above $40m/s$

Appendix C: CWEI

The CWEI has been calculated for various thresholds as presented in Table C1 and illustrated in Figure C1

https://doi.org/10.5194/egusphere-2025-3173
Preprint. Discussion started: 4 August 2025

Table C1. The cover for the various scenarios and periods of wind at different thresholds including CWEI.

	15 m/s					17.2 m/s					18 m/s					20 m/s				
	−1° C	Ref	+1° C	+2° C	+3° C	−1° C	Ref	+1° C	+2° C	+3° C	−1° C	Ref	+1° C	+2° C	+3° C	−1° C	Ref	+1° C	+2° C	+3° C
1 Hour	5.71 %	6.34 %	8.77 %	7.08 %	7.52 %	9.92 %	9.45 %	9.93 %	9.55 %	9.19 %	10.23 %	9.62 %	8.64 %	9.76 %	7.87 %	9.50 %	8.84 %	7.09 %	9.50 %	6.79 %
2 Hours	14.38 %	13.59 %	12.17 %	11.42 %	10.62 %	10.61 %	9.86 %	7.16 %	8.73 %	7.65 %	8.26 %	7.93 %	6.06 %	7.56 %	6.85 %	6.70 %	6.35 %	6.21 %	7.57 %	6.63 %
3 Hours	7.46 %	7.36 %	5.35 %	7.87 %	7.68 %	4.19 %	4.35 %	3.82 %	4.26 %	5.31 %	4.19 %	4.39 %	4.61 %	5.13 %	5.70 %	6.57 %	7.07 %	7.57 %	7.95 %	8.67 %
4 Hours	4.72 %	4.41 %	4.31 %	5.15 %	5.42 %	5.75 %	5.09 %	5.01 %	6.22 %	6.46 %	8.90 %	7.66 %	7.60 %	7.68 %	8.36 %	8.77 %	9.22 %	9.69 %	10.09 %	10.64 %
5 Hours	5.52 %	5.27 %	5.07 %	4.89 %	4.77 %	14.64 %	13.98 %	14.18 %	12.17 %	10.66 %	15.29 %	15.36 %	15.54 %	13.25 %	12.14 %	11.89 %	11.08 %	10.22 %	9.58 %	8.72 %
6 Hours	6.17 %	5.55 %	5.48 %	5.46 %	5.33 %	9.16 %	9.25 %	9.69 %	9.07 %	10.97 %	6.89 %	7.25 %	7.33 %	9.01 %	9.81 %	1.85 %	2.02 %	2.06 %	2.56 %	2.46 %
7 Hours	6.12 %	5.99 %	6.63 %	6.78 %	7.06 %	5.91 %	6.53 %	6.12 %	8.63 %	7.27 %	3.40 %	3.47 %	3.44 %	4.91 %	4.14 %	1.26 %	1.24 %	1.39 %	1.18 %	1.35 %
8 Hours	6.54 %	7.05 %	8.48 %	6.59 %	7.52 %	2.56 %	2.82 %	3.22 %	3.32 %	3.16 %	1.49 %	1.59 %	1.74 %	1.87 %	1.81 %	0.71 %	0.80 %	0.83 %	1.05 %	0.89 %
9 Hours	6.28 %	6.56 %	6.65 %	7.26 %	6.94 %	1.59 %	1.32 %	1.75 %	1.73 %	1.86 %	1.02 %	0.92 %	1.30 %	0.94 %	1.11 %	0.69 %	0.55 %	0.68 %	0.72 %	0.75 %
10+ Hours	24.14 %	24.32 %	22.49 %	25.93 %	24.83 %	6.19 %	6.47 %	6.15 %	6.92 %	6.78 %	4.44 %	4.63 %	4.39 %	4.95 %	4.79 %	1.57 %	1.63 %	1.56 %	1.73 %	1.76 %
Cover	86.93 %	86.44 %	85.42 %	88.44 %	87.70 %	70.53 %	69.12 %	67.02 %	70.60 %	69.30 %	64.11 %	62.82 %	60.65 %	65.08 %	62.59 %	49.50 %	48.81 %	47.31 %	51.93 %	48.66 %
CWEI	56350	56402	55078	58343	57614	35175	35080	34769	37131	36552	29799	29646	29542	31618	30978	19583	19406	19302	20350	19881

	21 m/s					22 m/s					23 m/s					24.5 m/s				
	−1° C	Ref	+1° C	+2° C	+3° C	−1° C	Ref	+1° C	+2° C	+3° C	−1° C	Ref	+1° C	+2° C	+3° C	−1° C	Ref	+1° C	+2° C	+3° C
1 Hour	9.04 %	8.35 %	7.29 %	9.02 %	7.06 %	8.16 %	7.52 %	7.70 %	7.76 %	6.98 %	7.88 %	7.46 %	7.30 %	7.03 %	6.74 %	5.84 %	5.69 %	6.75 %	6.66 %	6.38 %
2 Hours	6.10 %	5.65 %	5.59 %	7.43 %	5.83 %	5.67 %	5.55 %	4.81 %	6.69 %	5.60 %	4.86 %	4.97 %	4.58 %	5.92 %	5.66 %	3.52 %	3.58 %	4.47 %	5.01 %	4.26 %
3 Hours	6.87 %	7.26 %	8.31 %	7.88 %	9.74 %	5.60 %	6.15 %	7.91 %	6.93 %	9.04 %	4.96 %	4.93 %	7.95 %	6.76 %	7.88 %	3.34 %	3.40 %	5.75 %	4.74 %	5.39 %
4 Hours	7.92 %	9.15 %	9.08 %	10.33 %	9.70 %	8.18 %	8.78 %	8.04 %	9.89 %	8.85 %	6.92 %	7.26 %	5.94 %	7.01 %	5.83 %	4.32 %	3.94 %	3.05 %	3.34 %	3.26 %
5 Hours	7.92 %	6.96 %	6.51 %	5.42 %	5.58 %	4.21 %	3.58 %	3.70 %	2.64 %	2.65 %	1.93 %	1.99 %	1.85 %	1.74 %	1.99 %	1.03 %	0.98 %	1.04 %	1.12 %	1.29 %
6 Hours	1.32 %	1.25 %	1.31 %	1.53 %	1.37 %	1.10 %	1.06 %	1.15 %	1.17 %	1.09 %	0.90 %	0.92 %	0.87 %	0.89 %	1.00 %	0.51 %	0.67 %	0.51 %	0.63 %	0.60 %
7 Hours	1.07 %	0.91 %	1.21 %	1.10 %	1.02 %	0.85 %	0.93 %	0.92 %	1.04 %	0.95 %	0.59 %	0.65 %	0.59 %	0.76 %	0.51 %	0.08 %	0.10 %	0.18 %	0.29 %	0.22 %
8 Hours	0.68 %	0.74 %	0.62 %	0.72 %	0.75 %	0.45 %	0.48 %	0.41 %	0.36 %	0.42 %	0.17%	0.11 %	0.20 %	0.21 %	0.24 %	0.02 %	0.01 %	0.06 %	-	0.08 %
9 Hours	0.40 %	0.41 %	0.46 %	0.34 %	0.53 %	0.28 %	0.19 %	0.22 %	0.21 %	0.25 %	0.13 %	0.02 %	0.12 %	0.08 %	0.15 %	-	-	-	-	0.02 %
10+ Hours	0.69 %	0.76 %	0.68 %	0.90 %	0.90 %	0.16 %	0.21 %	0.27 %	0.30 %	0.44 %	0.02 %	0.02 %	0.01 %	0.03 %	0.11 %	-	-	-	-	-
Cover	42.01 %	41.43 %	41.07 %	44.67 %	42.47 %	34.65 %	34.43 %	35.14 %	36.98 %	36.28 %	28.35 %	28.34 %	29.39 %	30.43 %	30.11 %	18.65 %	18.37 %	21.81 %	21.78 %	21.51 %
CWEI	15368	15265	15308	15941	15881	11755	11747	11993	12377	12434	8759	8810	9096	9500	9444	5256	5191	5895	5954	6035

https://doi.org/10.5194/egusphere-2025-3173
Preprint. Discussion started: 4 August 2025

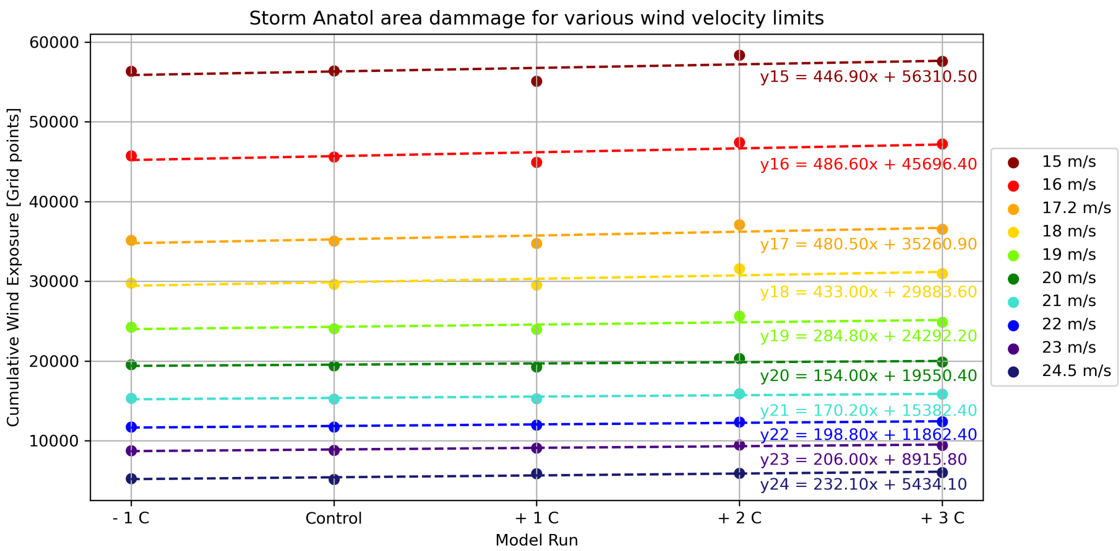

Figure C1. Development of the CWEI for the 5 model scenarios

Appendix D: Required Software and Dependencies

The following Python libraries and tools were used to access and process the data, along with the specific versions employed in this study:

cfgrib, version 0.9.10.4

365 ecCodes, version 1.5.0

xarray, version 2023.7.0

These constitute the minimum requirements necessary to handle the GRIB-formatted data used in the analysis. These libraries themselves have additional dependencies, which are typically resolved automatically when using standard installation tools.

370 *Author contributions.* JKHØ: Formal analysis, Writing original draft, Investigation, conceptualization. JHC: Conceptualization, Review/editing. RMKZ: Coding, DINI/trajectory plot, Analysis, Review/editing. HV: Conceptualization, Review/editing. HF: HARMONIE-AROME simulations, Review/editing.

Competing interests. The authors declare that they have no conflict of interest.

https://doi.org/10.5194/egusphere-2025-3173
Preprint. Discussion started: 4 August 2025

Acknowledgements. This work was supported by the Realdania Philanthropy project PRJ-2021-00176 “Metoder til klimatilpasning af det byggede miljø”. JKHØ acknowledge the support of the Danish government through the National Center for Climate Research (NCKF) Artificial intelligence tools (specifically ChatGPT by OpenAI) were used to assist in improving the clarity and wording of parts of the manuscript. All content was reviewed and verified by the authors.

https://doi.org/10.5194/egusphere-2025-3173
Preprint. Discussion started: 4 August 2025

References

Andrée, E., Su, J., Larsen, M. A. D., Madsen, K. S., and Drews, M.: Simulating major storm surge events in a complex coastal region, Ocean Modelling, 162, 101 802, https://doi.org/https://doi.org/10.1016/j.ocemod.2021.101802, 2021.

Bengtsson, L., I., H. K., and Keenlyside, N.: Will extratropical storms intensify in a warmer climate, Journal of climate, 22, 2276–2301, https://doi.org/10.1175/2008JCLI2678.1, 2009.

Bengtsson, L., Andrae, U., Aspelien, T., Batrak, Y., Calvo, J., De Roy, W., Gleeson, E., Hansen-Sass, B., Homleid, M., Hortal, M., Ivarsson, K., Lenderink, G., Niemelä, S., Nielsen, C. P., Onvlee, J., Rontu, L., Samuelsson, P., Munoz, D. S., Subias, A., Tijm, S., Toll, V., Yang, X., and Køltzow, M. : The HARMONIE-AROME Model Configuration in the ALADINE-HIRLAM NWP System, Monthly Weather Review, 145, 1919–1935, 2017.

Brogli, R., Heim, C., Mensch, J., Sørland, S. L., and Schär, C.: The pseudo-global-warming (PGW) approach: methodology, software package PGW4ERA5 v1.1, validation, and sensitivity analyses, Geoscientific Model Development, 16, 907–926, https://doi.org/10.5194/gmd-16-907-2023, 2023.

Cappelen, J., Olufsen, S., Ribergaard, M. H., Nielsen, J. W., Schmith, T., and Hansen, N.: Decemberorkanen 1999, https://www.dmi.dk/vejr-og-atmosfare/temaforside-decemberorkanen-1999, 2018.

Catto, J. L.: Extratropical cyclone classification and its use in climate studies, Reviews of Geophysics, 54, 486–520, https://doi.org/https://doi.org/10.1002/2016RG000519, 2016.

Chang, E. K.-M., Yau, A. M.-W., and Zhang, R.: Finding Storm Track Activity Metrics That Are Highly Correlated with Weather Impacts. Part II: Estimating Precipitation Change Associated with Projected Storm Track Change over Europe, Journal of Climate, 35, 2423 – 2440, https://doi.org/10.1175/JCLI-D-21-0259.1, 2022.

Christensen, J. H. and Christensen, O. B.: Severe summertime flooding in Europe], Nature, 421, 805, 2003.

Ciullo, A., Martius, O., Strobl, E., and Bresch, D. N.: A framework for building climate storylines based on downward counterfactuals: The case of the European Union solidarity fund, Climate Risk Management, 33, 100 349, https://doi.org/10.1016/j.crm.2021.100349, 2021.

Della-Marta, P. M. and Pinto, J. G.: Statistical uncertainty of changes in winter storms over the North Atlantic and Europe in an ensemble of transient climate simulations, Geophysical Research Letters, 36, https://doi.org/https://doi.org/10.1029/2009GL038557, 2009.

Donat, M. G., Leckebusch, G. C., and Ulbrich, U.: Future changes in European winter storm losses and extreme wind speeds inferred from GCM and RCM multi-model simulations, Natural Hazards and Earth System Sciences, 11, 1351–1370, https://doi.org/https://doi.org/10.5194/nhess-11-1351-2011, 2011a.

Donat, M. G., Pardowitz, T., Leckebusch, G. C., Ulbrich, U., and Burghoff, O.: High-resolution refinement of a storm loss model and estimation of return periods of loss-intensive storms over Germany, Natural Hazards and Earth System Sciences, 11, 2821–2833, https://doi.org/https://doi.org/10.5194/nhess-11-2821-2011, 2011b.

Eady, E.: Long Waves and Cyclone Waves, Tellus, 1:3, 1–71, https://doi.org/10.1111/j.2153-3490.1949.tb01265.x, 1949.

EUROCODE: EN 1991-1-4: Eurocode 1: Actions on structures – Part 1-4: General actions – Wind actions, reprinted 2015, 2005.

Federer, M., Papritz, L., Sprenger, M., and Grams, C. M.: Synoptic perspective on the conversion and maintenance of local available potential energy in extratropical cyclones, Weather and Climate Dynamics, 6, 211–230, https://doi.org/10.5194/wcd-6-211-2025, 2025.

Feser, F., Barcikowska, M., Krueger, O., Schenk, F., Weisse, R., and Xia, L.: Storminess over the North Atlantic and northwestern Europe – A review, Quarterly Journal of the Royal Meteorological Society, 141, 350–382, https://doi.org/10.1002/qj.2364, 2015.

https://doi.org/10.5194/egusphere-2025-3173
Preprint. Discussion started: 4 August 2025

Fink, A. H., Pohle, S., Pinto, J. G., and Knippertz, P.: Diagnosing the influence of diabatic processes on the explosive deepening of extratropical cyclones, Geophysical Research Letters, 39:7, https://doi.org/10.1029/2012GL051025, 2012.

Fischer, E. M. and Knutti, R.: Anthropogenic contribution to global occurrence of heavy-precipitation and high-temperature extremes, Nature climate change, 5, 560–565, 2015.

Gastineau, G. and Soden, B. J.: Model projected changes of extreme wind events in response to global warming, Geophysical research letters, 36, https://doi.org/10.1029/2009GL037500, 2009.

Gliksman, D., Averbeck, P., Becker, N., Gardiner, B., Goldberg, V., Grieger, J., Handorf, D., Haustein, K., Karwat, A., Knutzen, F., Lentink, H. S., Lorenz, R., Niermann, D., Pinto, J. G., Queck, R., Ziemann, A., and Franzke, C. L. E.: Review article: A European perspective on wind and storm damage – from the meteorological background to index-based approaches to assess impacts, Natural Hazards and Earth System Sciences, 23, 2171–2201, https://doi.org/10.5194/nhess-23-2171-2023, 2023.

Grinsted, A., Ditlevsen, P., and Christensen, J.: Normalized US hurricane damage estimates using area of total destruction, PNAS, 48, https://doi.org/10.1073/pnas.1912277116, 2019.

Hawkins, E., Compo, G. P., and Sardeshmukh, P. D.: ESD Ideas: Translating historical extreme weather events into a warmer world, Earth System Dynamics, 14, 1081–1084, https://doi.org/10.5194/esd-14-1081-2023, 2023.

Hersbach, H., Bell, B., Berrisford, P., Hirahara, S., Horányi, A., Muñoz-Sabater, J., Nicolas, J., Peubey, C., Radu, R., Schepers, D., Simmons, A., Soci, C., Abdalla, S., Abellan, X., Balsamo, G., Bechtold, P., Biavati, G., Bidlot, J., Bonavita, M., De Chiara, G., Dahlgren, P., Dee, D., Diamantakis, M., Dragani, R., Flemming, J., Forbes, R., Fuentes, M., Geer, A., Haimberger, L., Healy, S., Hogan, R. J., Hólm, E., Janisková, M., Keeley, S., Laloyaux, P., Lopez, P., Lupu, C., Radnoti, G., de Rosnay, P., Rozum, I., Vamborg, F., Villaume, S., and Thépaut, J.-N.: The ERA5 global reanalysis, Quarterly Journal of the Royal Meteorological Society, 146, 1999–2049, https://doi.org/https://doi.org/10.1002/qj.3803, 2020.

Hibino, K., Takayabu, I., Wakazuki, Y., and Ogata, T.: Physical responses of convective heavy rainfall to future warming condition: Case study of the Hiroshima event, Frontiers in Earth Science, 6, 35, https://doi.org/10.3389/feart.2018.00035, 2018.

IPCC: Framing, Context and Methods, chap. 1, pp. 1–60, Cambridge University Press, https://doi.org/10.1017/9781009157896.001, 2021a.

IPCC: Climate Scenarios and Model Experiments, chap. 4, pp. 140–200, Cambridge University Press, https://doi.org/10.1017/9781009157896.006, 2021b.

IPCC: Weather and Climate Extreme Events in a Changing Climate, chap. 11, pp. 1513–1766, Cambridge University Press, https://doi.org/10.1017/9781009157896.013, 2021.

Kettle, A. J.: Storm Anatol over Europe in December 1999: impacts on societal and energy infrastructure, Advances in Geosciences, 56, 141–153, https://doi.org/10.5194/adgeo-56-141-2021, 2021.

Klawa, M. and Ulbrich, U.: A model for the estimation of storm losses and the identification of severe winter storms in Germany, Natural Hazards and Earth system sciences, 3, 725–732, 2003.

Laurila, T. K., Gregow, H., Cornér, J., and Sinclair, V. A.: Characteristics of extratropical cyclones and precursors to windstorms in northern Europe, Weather and Climate Dynamics, 2, 1111–1130, https://doi.org/10.5194/wcd-2-1111-2021, 2021.

Leckebusch, G. C., Renggli, D., and Ulbrich, U.: Development and application of an objective storm severity measure for the Northeast Atlantic region, Meteorologische Zeitschrift, 17, 575–587, https://doi.org/10.1127/0941-2948/2008/0323, 2008.

Li, M., Woollings, T., Hodges, K., and Masato, G.: Extratropical cyclones in a warmer, moister climate: A recent Atlantic analogue, Geophysical Research Letters, 41, 8594–8601, https://doi.org/https://doi.org/10.1002/2014GL062186, 2014.

https://doi.org/10.5194/egusphere-2025-3173
Preprint. Discussion started: 4 August 2025

Lindsey, R. and Dahlman, L.: Climate Change: Global Temperature, NOAA Climate.gov, https://www.energy.gov/sites/default/files/2024-06/133

Little, A. S., Priestley, M. D. K., and Catto, J. L.: Future increased risk from extratropical windstorms in northern Europe, Nature communications, https://doi.org/10.1038/s41467-023-40102-6, 2023.

Lorenz, R., Becker, N., Gardiner, B., Ulbrich, U., Hanewinkel, M., and Benjamin, S.: Storm damage beyond wind speed – Impacts of wind characteristics and other meteorological factors on tree fall along railway lines, EGUsphere, 2024, 1–34, https://doi.org/10.5194/egusphere-2024-120, 2024.

Lynn, B. A. and Stathopoulos, T.: Wind-induced fatigue on low metal buildings., Journal of structural Engineering, 11, 826–839, 1985.

Matte, D., Christensen, J. H., Feddersen, H., Vedel, H., Nielsen, N. W., Pedersen, R. A., and Zeitzen, R. M. K.: On the potentials and limitations of Attributing a Small-Scale Climate event, Geophysical Research Letters, 49, https://doi.org/10.1029/2022GL099481, 2022.

Neu, H. J. A.: Interannual Variations and Longer-Term changes in the Sea State of the North Atlantic From 1970 to 1982, Journal of Geophysical Research, 89, 6397–6402, 1984.

Nielsen, N. W. and Sass, B. H.: A numerical, high-resolution study of the life cycle of the severe storm over Denmark on 3 December 1999, Tellus A: Dynamic Meteorology and Oceanography, 55A, 2003.

Nilsson, C., Goyette, S., and Bärring, L.: Relating forest damage data to the wind field from high-resolution RCM simulations: Case study of Anatol striking Sweden in December 1999, Global and Planetary Change, 57, 161–176, https://doi.org/https://doi.org/10.1016/j.gloplacha.2006.11.011, extreme Climatic Events, 2007.

Philip, S., Kew, S., van Oldenborgh, G. J., Otto, F., Vautard, R., van der Wiel, K., King, A., Lott, F., Arrighi, J., Singh, R., and van Aalst, M.: A protocol for probabilistic extreme event attribution analyses, Advances in Statistical Climatology, Meteorology and Oceanography, 6, 177–203, https://doi.org/10.5194/ascmo-6-177-2020, 2020.

Prahl, B. F., Rybski, D., Kropp, J. P., Burghoff, O., and Held, H.: Applying stochastic small-scale damage functions to German winter storms, Geophysical Research Letters, 39, https://doi.org/https://doi.org/10.1029/2012GL050961, 2012.

Priestley, M. D. K. and Catto, J. L.: Future changes in the extratropical storm tracks and cyclone intensity, wind speed, and structure, Weather and Climate Dynamics, 3, 337–360, https://doi.org/10.5194/wcd-3-337-2022, 2022.

Ruosteenoja, K., Vihma, T., and Venäläinen, A.: Projected Changes in European and North Atlantic Seasonal Wind Climate Derived from CMIP5 Simulations, Journal of Climate, 32, 6467 – 6490, https://doi.org/10.1175/JCLI-D-19-0023.1, 2019.

Schär, C., Frei, C., Lüthi, D., and Davies, H. C.: Surrogate climate-change scenarios for regional climate models, Geophysical Research Letters, 23, 669–672, https://doi.org/https://doi.org/10.1029/96GL00265, 1996.

Severino, L. G., Kropf, C. M., Afargan-Gerstman, H., Fairless, C., de Vries, A. J., Domeisen, D. I. V., and Bresch, D. N.: Projections and uncertainties of winter windstorm damage in Europe in a changing climate, Natural Hazards and Earth System Sciences, 24, 1555–1578, https://doi.org/10.5194/nhess-24-1555-2024, 2024.

Shepherd, T., Boyd, E., Calel, R., Chapman, S. C., Dessai, S., Dima-West, I. M., Fowler, H. J., James, R., Maraun, D., Martius, O., Senior, C. A., Sobel, A. H., Stainforth, D. A., Tett, S. F. B., Trendberth, K. E., van der Hurk, B. J. J. M., Watkins, N. W., Wilby, R. L., and Zenghelis, D. A.: Storylines: an alternative approach to representing uncertainty in physical aspects of climate change., Climatic Change, 151, 555–571, https://doi.org/10.1007/s10584-018-2317-9, 2018.

Shepherd, T. G.: Storyline approach to the construction of regional climate change information, Proceedings of the Royal Society A: Mathematical, Physical and Engineering Sciences, 475, 20190 013, https://doi.org/10.1098/rspa.2019.0013, 2019.

https://doi.org/10.5194/egusphere-2025-3173
Preprint. Discussion started: 4 August 2025

Sillmann, J., Shepherd, T. G., van den Hurk, B., Hazeleger, W., Martius, O., Slingo, J., and Zscheischler, J.: Event-Based Storylines to Address Climate Risk, Earth's Future, 9, e2020EF001 783, https://doi.org/https://doi.org/10.1029/2020EF001783, e2020EF001783 2020EF001783, 2021.

Souto-Ceccon, P. E., Montes, J., Duo, E., Ciavola, P., Fernández-Montblanc, T., and Armaroli, C.: A European database of resources on coastal storm impacts, Earth System Science Data, 17, 1041–1054, https://doi.org/10.5194/essd-17-1041-2025, 2025.

The WASA Group: Changing waves and storms in the Northeast Atlantic?, Bulletin of the American Meteorological Society, 79, 1998.

Trenberth, K. E., Fasullo, J. T., and Shepherd, T. G.: Attribution of climate extreme events, Nature climate change, 5, 725–730, https://doi.org/10.1038/NCLIMATE2657, 2015.

Ulbrich, U., Fink, A. H., Klawa, M., and Pinto, J. G.: Three extreme storms over Europe in December 1999, Weather, 56, 70–80, https://doi.org/https://doi.org/10.1002/j.1477-8696.2001.tb06540.x, 2001.

Ulbrich, U., Leckebusch, G. C., and Pinto, J. G.: Extra-tropical cyclones in the present and future climate: a review., Theoretical and Applied Climatology, 96, 117–131, https://doi.org/10.1007/s00704-008-0083-8, 2009.

Voldborg, H.: Vredens julemåned, Vejret, 82, 1–7, 2000.

von Storch, H., Feser, F., Haeseler, S., Lefebvre, C., and Stendel, M.: A violent midlatitude storm in Northern Germany and Denmark, 28 October 2013 [in "Explaning Extremes of 2013 from a Climate Perspective"], Bull. Amer. Meteor. Soc., 95, 76–78, 2014.

Wang, J., Liu, Y., and Zhang, Z.: Fatigue Damage and Reliability Assessment of Wind Turbine Structure During Service Utilizing Real-Time Monitoring Data., Buildings, 14, https://doi.org/https://doi.org/10.3390/buildings14113453, 2024.

Woth, K., Weisse, R., and von Storch, H.: Climate change and North Sea storm surge extremes: an ensemble study of storm surge extremes expected in a changed climate projected by four different regional climate models., Ocean Dynamics, 56, 3–15, https://doi.org/https://doi.org/10.1007/s10236-005-0024-3, 2005.

Zeitzen, R. M. K., Christensen, J. H., Øelund, J. K. H., Feddersen, H., Vedel, H., Nielsen, N. W., and Matte, D.: Windstorm Extremes in a Warmer World: Raising the Bar for Destruction., Geophysical Research Letters, 52, https://doi.org/10.1029/2025GL115936, 2025.